CYBERNETICS AND PHYSICS, VOL. 14, NO. 3, 2025, 228–238

BREATHERS PROPAGATION IN THE GRANULAR LOCALLY RESONANT CHAINS ON ELASTIC FOUNDATION AND THEIR OSCILLATORY TAILS

Mikhail Kalmykov
Polymers and Composite Materials Department
N.N.Semenov Federal Research Center of Chemical Physics,
Russian Academy of Sciences,
Russia

Physics Department
HSE University
Russia

Margarita Kovaleva
Polymers and Composite Materials Department
N.N.Semenov Federal Research Center of Chemical Physics,
Russian Academy of Sciences,
Russia
makovaleva@chph.ras.ru
Physics Department
HSE University
Russia

Article history:
Received 14.08.2025, Accepted 20.11.2025

Abstract

The paper addresses the propagation of the breather in the quasi-one-dimensional model of locally resonant granular lattice metamaterial on the elastic foundation. The model is presented as a one-dimensional mass-in-mass chain with Hertzian type of nearest-neighbor interaction and linear coupling with the inner elements. In the case of impact excitation on the side of the chain, we demonstrate the formation of the breathers. We consider two types of traveling breathers and detect their existence in a wide range of system parameters. We report that the propagation of the breather is accompanied by energy radiation to the oscillatory tails. Furthermore, we present an asymptotic analysis of the propagation and formulate the criteria for the absence of the energy loss of the breather.

Key words

locally-resonant granular chain, mass-in-mass model, breathers, oscillatory tails.

1 Introduction

Energy transfer in nonlinear chains has attracted the interest of researchers for decades [Vakakis et al., 2022]. It is closely connected with the study of the mechanisms of energy transfer and localization [Vorotnikov et al., 2018; Manevitch, 2018; Yacobi et al., 2019; Manevitch et al., 2016], nonlinear wave transition, and their stability [Kapitula et al., 2013]. Modern science and technology take advantage of the effects of local resonances to control energy transfer and construct media and systems with desired properties [Ma et al., 2016; Haberman et al., 2016; Deng et al., 2021; Roca et al., 2020; Zhou et al., 2023; Zega et al., 2020]. The main interest is focused on the metamaterials, or metastructures. Acoustic metamaterials are a promising and fundamentally important area of research for describing the energy-absorbing properties of materials and the possibilities of controlling wave dynamics in one-dimensional, two-dimensional, and three-dimensional systems. The aim of the research is to analyze the passage of waves and the energy transfer associated with breathers through such locally resonant chain structures. The analysis of the wave transition, their changes and redirection play a key role in understanding numerous phenomena in various fields of physics and technology[Bashar Esmail, 2022; Gantzounis et al., 2013; Yacobi et al., 2019; Smith et al., 2004]. One of the common types of models describing metamaterials are discrete nonlinear chains, for example, of a granular type[Gantzounis et al., 2013; Yacobi et al., 2019; Smith et al., 2004; Fang et al., 2025], especially with locally resonant inclusions[Gantzounis et al., 2013; Smith et al., 2004; Fang et al., 2025; Espinosa et al., 2024; Bonanomi et al., 2015; Kevrekidis et al., 2013]. Understanding the mechanisms of excitation propagation along quasi-one-dimensional, locally resonant granular systems or its localization in a certain domain of such a system is necessary both for describing structural features and for predicting the properties of final materials. We consider the model of a one-dimensional, locally resonant granular chain on the substrate subject to

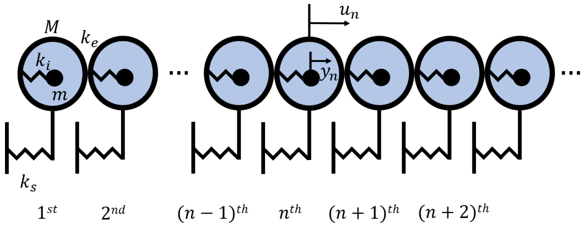

Figure 1. A one-dimensional, locally resonant chain of the mass-in-mass type on a substrate

the impact load on one side of the long chain. We show the existence of the traveling breathers accompanied by the oscillatory tails. Furthermore, we consider the two types of traveling breathers existing in the model. The effect of chain parameters on the breathers' transition is discussed, and different regimes of breathers' existence and their stability are studied numerically for different parameters ranges. The energy transfer is considered in connection with the properties of the chain. Using the Fourier representation, we find the anti-resonance condition for the oscillatory tails and formulate criteria for the system's parameters to eliminate the energy radiation of the breathers. The paper is organized as follows: Section 2 presents the system description and its basic properties. Section 3 demonstrates results of the numeric simulations. Section 4 is devoted to the analytical criteria of the absence of the oscillatory tails. In the Conclusions section we discuss the results.

2 The Model

The locally resonant structures are often modeled by the mass-in-mass oscillatory chains[Banerjee et al., 2019]. The mass-in-mass chains are widely considered in old and recent papers [Bonanomi et al., 2015; Kevrekidis et al., 2013; Banerjee et al., 2019; Huang et al., 2009; Rosenau et al., 2014; Kikot et al., 2022; Porubov, 2023]. The oscillatory chains with Hertzian type of interaction were thoroughly studied experimentally, numerically, and theoretically in numerous works [Gantzounis et al., 2013; Espinosa et al., 2024; Bonanomi et al., 2015; Kevrekidis et al., 2013; Jayaprakash et al., 2013; James, 2012; James et al., 2013; Kevrekidis et al., 2016; Xu et al., 2015; Liu et al., 2016; Wallen et al., 2017; Liu et al., 2016; Vorotnikov et al., 2018]. It was shown that the nonlinear waves can exist in such systems, and their form and stability were also discussed. However, the locally resonant granular chains on the substrate were not considered. It is known that the granular chains with elastic substrate without local resonances demonstrate standing and traveling nonlinear breathers [James, 2012; James et al., 2013; Starosvetsky et al., 2017; Hasan et al., 2013]. In our work, we present a study of the mass-in-mass model of the chain on the elastic substrate with Hertzian type of interaction between the 'outer' elements.

To describe the interaction between the outer granules, we will use the Hertzian potential. In accordance with Hertz's law, the contact force F of the approaching bodies depends nonlinearly on the distance δ:

$$F = k\delta^p,$$

where $k = 2\frac{(1-\mu^2)}{E}$ is elastic constant, μ is Poisson's ratio, E is the normal modulus of elasticity. For contact between two solid spherical surfaces $p = \frac{3}{2}$. We consider the chain without precompression. The outer granules of the system are located on an elastic substrate, and the strength of their interaction is linearly dependent on displacement, so the substrate is represented as an elastic spring with some known stiffness coefficient. The interaction of the outer granules with the corresponding internal elements is linear. The equations of motion look as follows:

$$\begin{aligned} M\ddot{u}_n &= k_e{(u_{n-1}-u_n)^p}_+ \\ &- k_e{(u_n-u_{n+1})^p}_+ - k_s u_n - k_i\left(u_n-y_n\right), \\ m\ddot{y}_n &= k_i\left(u_n-y_n\right), \end{aligned} \quad (1)$$

where $p = \frac{3}{2}$. M, m are the masses of internal and outer granules, respectively;k_e is coefficient of interaction of external granules with each other; k_s is coefficient of interaction of external granules with the substrate; k_i is coefficient of interaction of external granules with internal granules.

The subscript "+" means multiplication by the Heaviside function, which allows us to take into account that the interaction between the outer granules occurs only when they come closer:

$$\begin{aligned} {(u_{n-1}-u_n)^p}_+ &= \theta\left(u_{n-1}-u_n\right)\left(u_{n-1}-u_n\right)^p; \\ {(u_n-u_{n+1})^p}_+ &= \theta\left(u_n-u_{n+1}\right)\left(u_n-u_{n+1}\right)^p. \end{aligned}$$

To reduce the free parameters of the system, we will carry out normalization

$$\begin{aligned} \ddot{u}_n &= g{(u_{n-1}-u_n)^p}_+ \\ &- g{(u_n-u_{n+1})^p}_+ - u_n - k_1\left(u_n-y_n\right), \\ V_1\ddot{y}_n &= k_1\left(u_n-y_n\right), \end{aligned} \quad (2)$$

where $\frac{k_e}{m} = g; \frac{k_s}{m} = 1; \frac{k_i}{m} = k_1; V_1 = \frac{m}{M}$

3 Unit-cell model

To get some idea of the behavior of the system, we consider the effect of various parameters on the frequency of the system. To do this, let's consider a unit cell of the system, which can be described by the following system of equations:

$$\begin{aligned} \ddot{u} &= -u - k_1\left(u-y\right); \\ V_1\ddot{y} &= k_1\left(u-y\right). \end{aligned} \quad (3)$$

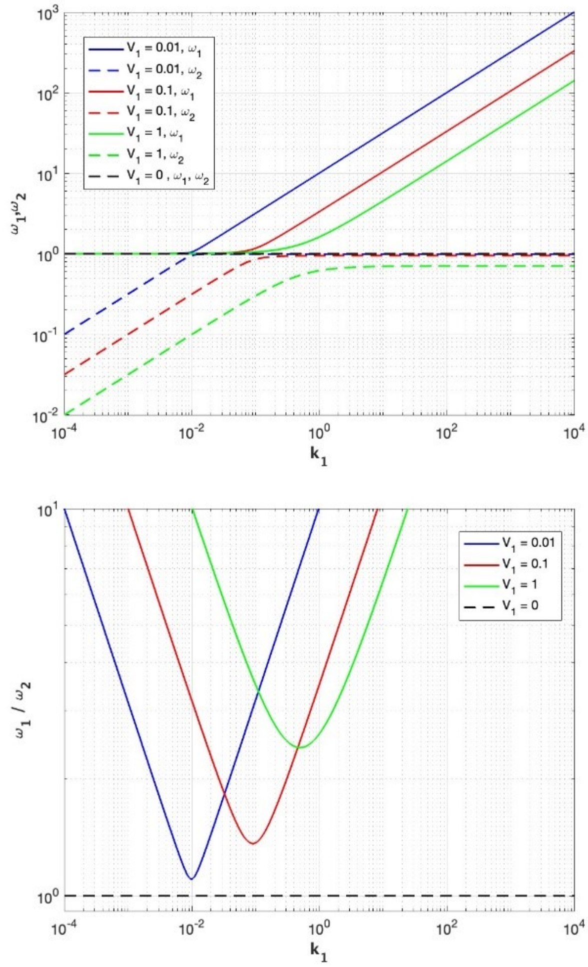

Figure 2. (a) Frequency of a single cell of the system, when the parameters of local resonance change; (b) the ratio of the system's frequencies

To obtain the dispersion relation, we substitute solutions in the form of a plane wave:

$$u = Ae^{i(kd-\omega t)};$$
$$y = Be^{i(kd-\omega t)},$$

then

$$V_1\omega^4 - \omega^2 \left(k_1 + V_1 + k_1 V_1\right) + k_1 = 0. \quad (4)$$

A similar result can be obtained if the original system of equations is linearized. The solution of the above characteristic equation gives two frequencies $\omega_1 > \omega_2 > 0$, which depend on the characteristics of the resonator V_1 and k_1. Figure 2(a) shows the frequencies ω_1, ω_2 depending on local parameter k_1 for different values of V_1. Our study of the linear spectrum is in good agreement with the presented in [Bukhari et al., 2023]. However, for clarity, we present here the main features of the spectrum. The two different normal modes are evidently seen from Fig. 2(a) when the mass-ratio V_1 is not zero. The case when $V_1 = 0$ corresponds to a one-dimensional discrete oscillatory chain considered, for example, in [Mojahed et al., 2020]. The modes hybridization leads to the appearance of the band gap where no linear waves can exist. The frequency ratios of the two modes can change drastically for different values of V_1 and k_1, see Fig.2(b), having the minima for moderate values of k_1. For smaller values of k_1 the mode with higher frequency ω_1, corresponds to the out-of-phase motion with frequency close to unity; this behavior is asymptotically close to the motion of the discrete chain of masses without local resonances. It serves as the upper boundary of the isolation zone. The lower frequency ω_2 is the typical in-phase mode, its value is close to the frequency of the acoustic waves in the rigid body, and it serves as the upper boundary of the isolation zone. With an increase of k_1 one can see the transition between the modes. For larger values of k_1, the second mode becomes the lower boundary of the isolation zone, which is close to the fast frequency of a one-dimensional discrete chain without local resonators, while the first mode frequency increases with the growth of k_1.

4 Numerical simulation results

As mentioned in many studies, nonlinear waves play an essential role in signal processing, energy transfer, and localization in granular acoustical metamaterials [James et al., 2013; Kevrekidis et al., 2016; Xu et al., 2015; Liu et al., 2016; Wallen et al., 2017; Liu et al., 2016; Vorotnikov et al., 2018; Bonanomi et al., 2015; Starosvetsky et al., 2017; Hasan et al., 2013; Bukhari et al., 2023; Wattis, 2022; English et al., 2005]. One-dimensional granular chains with internal resonators can support propagation of breathers. A breather is a localized nonlinear wave with an internal degree of freedom. One-dimensional granular chains of the mass-in-mass type without a substrate have been well studied, the existence of breathers was considered [Liu et al., 2016; Wallen et al., 2017; Liu et al., 2016; Vorotnikov et al., 2018; Bonanomi et al., 2015; Starosvetsky et al., 2017; Hasan et al., 2013; Bukhari et al., 2023; Wattis, 2022; Hasan et al., 2015; James, 2012]. However, when a substrate is added, breathers become long-living, as they radiate energy into the oscillating tail. A similar observation was made for the granular, locally resonant chain without elastic foundation [Xu et al., 2015; **?**]. In this section, we demonstrate the traveling breathers in the oscillatory model mass-in-mass with elastic substrate for different ranges of parameters. The system of equations (2) was solved numerically using the Runge-Kutt method (ode45 function in MATLAB Software). The chain was taken long enough to study the transition of the waves without reflections. It was taken into account that the first and last outer elements are bounded by the wall, the interaction with it realized by the Hertzian potential with the same degree of nonlinearity. Depending

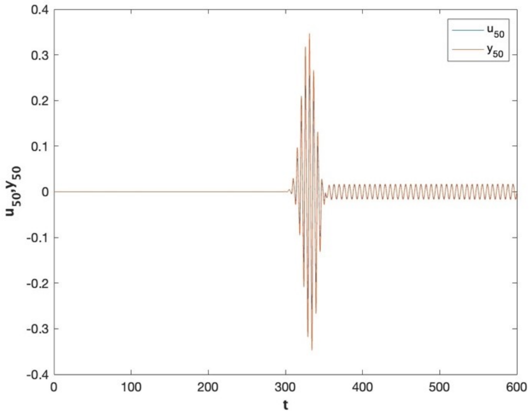

Figure 4. Temporal profile for the displacements of the outer and inner elements in the middle element of the chain for the travelling in-phase breather

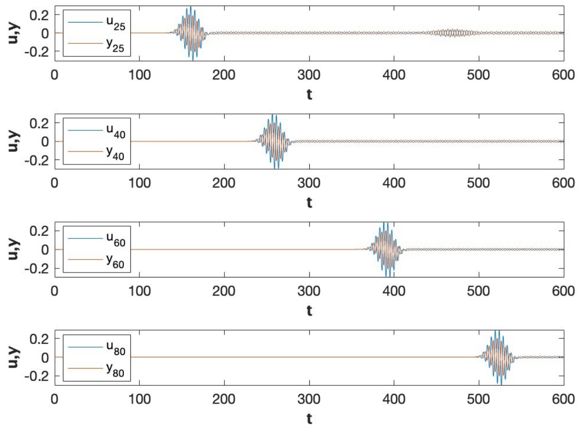

Figure 7. Spatial profiles for outer and inner elements during the transition of the breather for the parameters set: $g = 1; k_1 = 0.07; v_1 = 0.1$, initial conditions:$u_0\left(0\right) = 0.5$

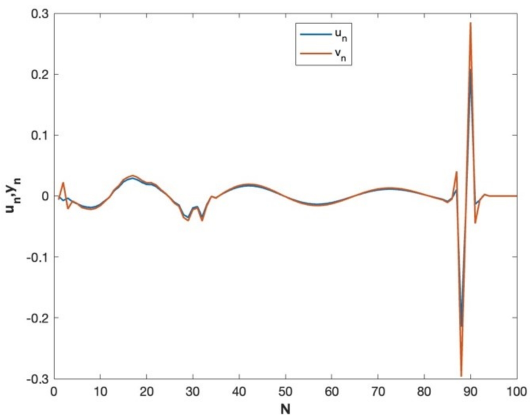

Figure 5. . Spatial profile for outer and inner elements in the middle-element of the chain for the travelling in-phase breather

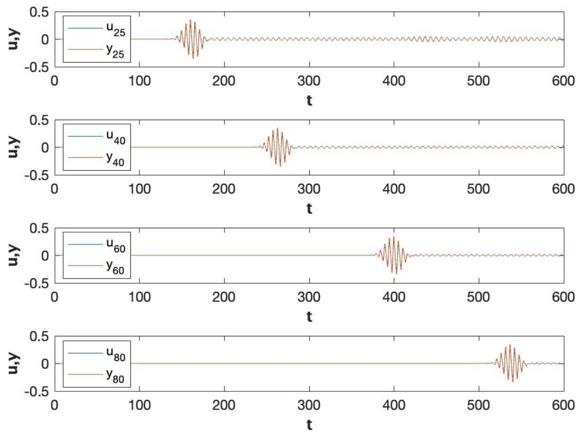

Figure 3. Spatial profiles for outer and inner elements during the transition of the in-phase breather for the parameters set: $g = 1; k_1 = 0.7; v_1 = 0.1$and initial conditions: $\dot{u}_1\left(0\right) = 0.5; \dot{y}_0\left(0\right) = 0.5$.

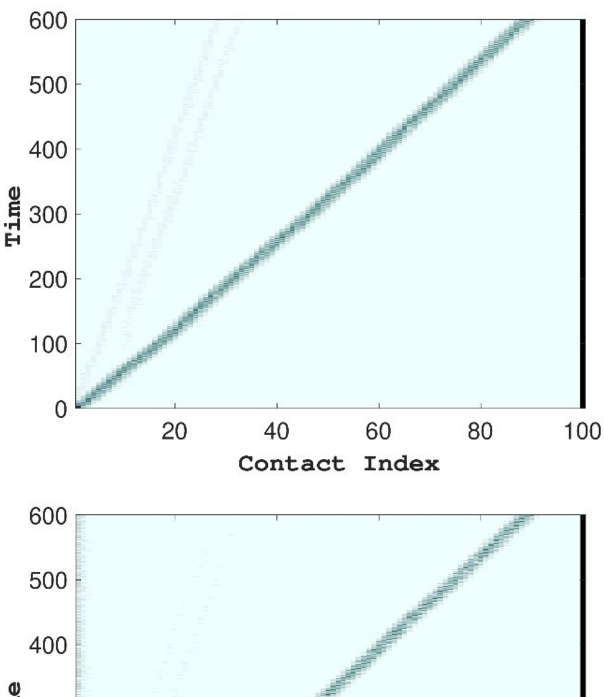

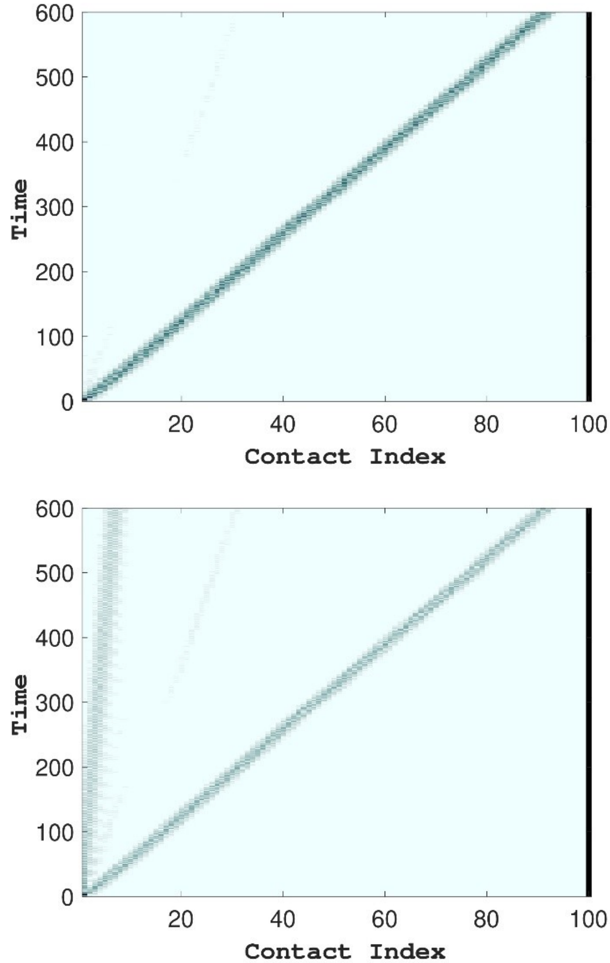

Figure 10. Spatiotemporal energy profiles of external (a) and internal (b) elements for the travelling anti-phase breather

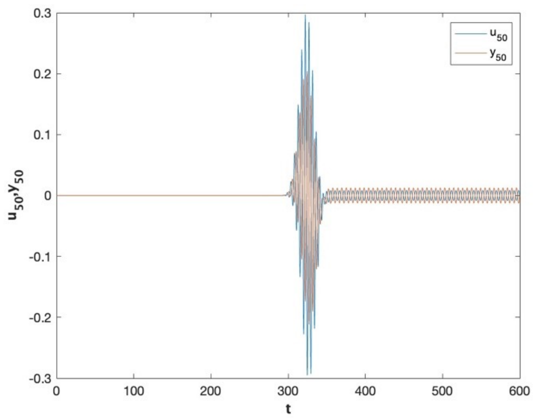

Figure 8. Temporal profile for the displacements of the outer and inner elements in the middle element of the chain for the travelling anti-phase breather

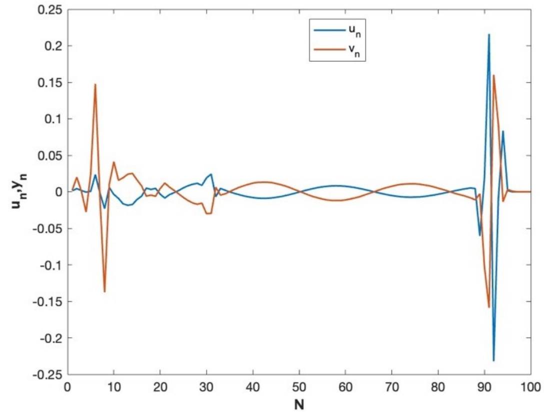

Figure 9. . Spatial profile for outer and inner elements in the middle-element of the chain for the travelling anti-phase breather

on the initial conditions, it is possible to obtain solutions in the form of traveling breathers. To obtain them, it is necessary to specify the initial displacements or pulses, the first granules of the chain, external, internal, or both at once. Figure 3 shows the temporal profiles of the outer (blue) and inner (orange) elements for the traveling breather demonstrating in-phase movement of the outer and inner elements. We call such breathers in-phase breathers for clarity. Figure 3 demonstrates the displacement of certain inner and outer granules over time. It can be seen that the breather moves along the chain almost without changing its amplitude and shape at a certain speed, and an oscillating tail spreads behind it. The same set of parameters and initial conditions is used to obtain Fig. 4, Fig.5, and Fig.6.

Let us consider Figure 6 with space-time energy profiles. An area coloured more intensely denotes greater energy. The dark line passing through the diagram corresponds to the breather, from which we can conclude that the breather carries the most energy in the system under consideration. Part of the breather's energy is radiated by the wave following the main pulse, which is commonly called an oscillatory tail. If the mass ratio V_1 is increased or the elastic ratio k_1 is decreased, the in-phase breathers become significantly unstable, and the out-of-phase travelling breathers can be considered. Figure 7 shows the temporal profiles of the outer (blue) and inner (orange) out-of-phase breathers. Similar to the in-phase breathers, they can propagate along the chain almost at a certain speed, and an oscillating tail spreads behind it. However, the dynamics of the inner and outer elements appears to be out-of-phase. The same set of parameters and initial conditions is used to obtain Fig. 8,Fig.9 and Fig.10.

As can be seen from Figure 9, in the wake of out-of-phase breathers propagating through the granular chain, there may be breathers of a smaller amplitude in a bound state. The interaction between them occurs in a nonlinear way, through an oscillating tail. This phenomenon requires additional research, which is not the subject of

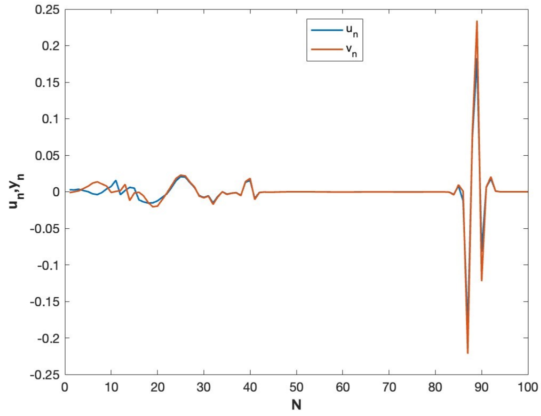

Figure 13. . Spatial profile for outer and inner elements in the middle-element of the chain. Parameters and initial conditions same as in Fig.11

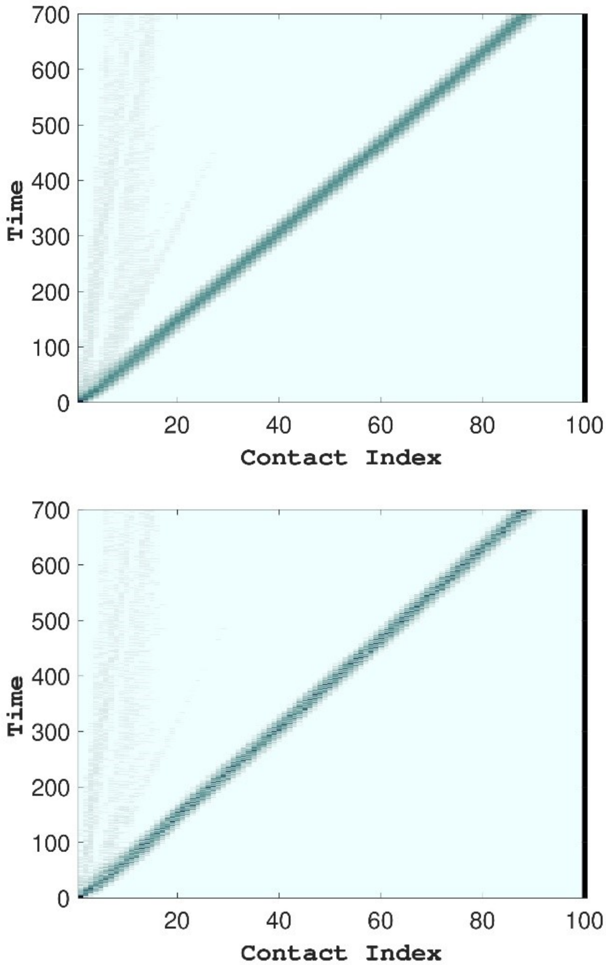

Figure 14. Spatiotemporal energy profiles of external (a) and internal (b) elements for the travelling breather. Parameters and initial conditions same as in Fig.11

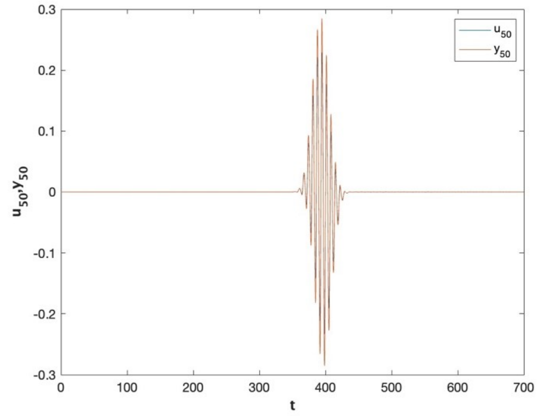

Figure 11. Temporal profile for the displacement of the outer and inner elements in the middle-element of the chain for the parameters set:$g = 1.5; k_1 = 4.7; v_1 = 1$, initial conditions: $\dot{u}_1(0) = 0.4; \dot{y}_0(0) = 0.5.$

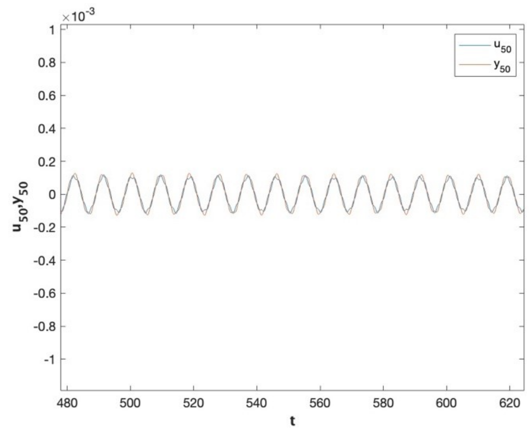

Figure 12. Oscillating tail of the breather. Parameters and initial conditions same as in Fig.11

current work. However, it is not possible to achieve their complete absence empirically, so in the next chapter we will consider an analytical method for finding the conditions for the propagation of breathers without oscillating tails, that is, the anti-resonance condition.

5 Anti-resonance condition

In this section we make a study on parameters of the system for the anti-resonance condition which should exclude the existence of oscillating tails of the traveling breathers. To achieve the non-radiating solution, we look for the anti-resonance condition similar to [Xu et al., 2015; English et al., 2005]. For convenience, we renormalize the initial system of equations (1) as follows:

$$\frac{k_1}{m} = 1; \frac{k_2}{m} = \widetilde{k_2}; \frac{k_3}{m} = k_1; V_1 = \frac{M}{m}$$

For brevity, let us omit the tilde over the coefficients , then the system of equations will take the form:

$$\begin{aligned} \ddot{u}_n = (u_{n-1} - u_n)^p{}_+ \\ -(u_n - u_{n+1})^p{}_+ - k_2 u_n - k_1 (u_n - y_n), \\ V_1 \ddot{y}_n = -k_1 (y_n - u_n). \end{aligned} \quad (5)$$

Let's focus on solutions in the form of a traveling wave in the following form:

$$\begin{aligned} u_n(t) = r(n - ct) = r(\xi) \\ v_n(t) = r(n - ct) = s(\xi). \end{aligned} \quad (6)$$

Now we transform the system to relative displacement variables or strain variables, which can be defined as follows

$$\begin{aligned} R(\xi) = r(\xi - 1) - r(\xi) \\ S(\xi) = s(\xi - 1) - s(\xi). \end{aligned} \quad (7)$$

The equations take the form:

$$\begin{aligned} c^2 \ddot{R}(\xi) = (R(\xi+1))_+^p + (R(\xi-1))_+^p - 2(R(\xi))_+^p \\ -k_2 R(\xi) - k_1 (R(\xi) - S(\xi)), \\ c^2 V_1 \ddot{S}(\xi) = -k_1 (S(\xi) - R(\xi)). \end{aligned} \quad (8)$$

We will follow the approach of [Bonanomi et al., 2015], rewriting the problem in Fourier space (upon a Fourier transform) and seeking fixed points of that problem upon inverse Fourier transform, similarly to [Bonanomi et al., 2015; Vorotnikov et al., 2018]. The details of the finite-domain scheme of the Fourier transform for the localized solutions are discussed in detail in [Huang et al., 2009], we proceed to the consideration of the finite-domain Fourier transform. The following Fourier series representation is valid: $\xi \in [-L, L]$:

$$f(\xi) = \sum_{k=-\infty}^{\infty} f_k e^{i \frac{2\pi}{2L} k\xi};$$

$$f_k = \frac{1}{2L} \int_{-L}^{L} f(\xi) e^{-i \frac{2\pi}{2L} k\xi} d\xi.$$

Consequently, the system of equations for Fourier images takes the form:

$$\begin{aligned} \left(k_1 + k_1 V_1 - c^2 V_1 \left(\frac{\pi}{L}\right)^2 k^2 - \frac{k_2 k_1}{c^2 \left(\frac{\pi}{L}\right)^2 k^2} + k_2 V_1 \right) \times \\ \times R_k = \\ = \frac{1}{c^2} \left(k_1 - c^2 V_1 \left(\frac{\pi}{L}\right)^2 k^2 \right) sinc^2 \left(\frac{\pi}{2L} k\right) (R_+^p)_k; \\ c^2 V_1 S_k \left(\frac{\pi}{L}\right)^2 k^2 = -k_1 (S_k - R_k). \end{aligned} \quad (9)$$

Note that

$$\begin{aligned} \int_{-L}^{L} \left[(R(\xi+1))_+^p + (R(\xi-1))_+^p - 2(R(\xi))_+^p \right] \times \\ \times e^{-i \frac{\pi}{L} k\xi} d\xi = -4 \sin^2 \left(\frac{\pi}{2L} k\right) (R_+^p)_k. \end{aligned}$$

For the resulting system of equations to be solvable, the following conditions are to be valid, which are the conditions of anti-resonance:

a)$k_{1p} = 2\pi n$; $k_{2p} = 2\pi m$ or $(R_+^p)_{1p,2p} = 0$;

b)$k_d = \frac{L}{\pi} \sqrt{\frac{k_1}{V_1 c^2}}$; $(R_+^p)_{k_d} = (R_+^p)_{-k_d}$;

where

$$\begin{aligned} k^2{}_{1p,2p} = \\ = \left(\frac{L}{\pi}\right)^2 \frac{1}{2V_1 c^2} ((k_1 + k_1 V_1 + k_2 V_1) \pm \\ \pm \sqrt{(k_1 + k_1 V_1 + k_2 V_1)^2 - 4 V_1 k_2 k_1}. \end{aligned}$$

We can rewrite the equation (9a) as follows:

$$\begin{aligned} R_k = \frac{1}{c^2} \frac{\left(k_1 - V_1 \left(c\frac{\pi}{L}\right)^2 k^2\right) \left(c\frac{\pi}{L}\right)^2 k^2}{\left(\left(\frac{\pi}{L}\right)^2 k^2 - k_{1p}^2\right) \left(\left(\frac{\pi}{L}\right)^2 k^2 - k_{2p}^2\right)} \times \\ \times sinc^2 \left(\frac{\pi}{2L} k\right) (R_+^p)_k. \end{aligned}$$

Using the notation:

$$\begin{aligned} M_{1k} = \frac{1}{c^2} \frac{\left(k_1 - V_1 \left(c\frac{\pi}{L}\right)^2 k^2\right) \left(c\frac{\pi}{L}\right)^2 k^2}{\left(\left(\frac{\pi}{L}\right)^2 k^2 - k_{1p}^2\right) \left(\left(\frac{\pi}{L}\right)^2 k^2 - k_{2p}^2\right)} \times \\ \times sinc^2 \left(\frac{\pi}{2L} k\right), \end{aligned}$$

we can rewrite the equation in the short form:

$$R_k = M_{1k} (R_+^p). \quad (10)$$

Knowing that the inverse Fourier transform of the product of the two images is equal to the convolution of the original functions, we perform the inverse transformation for M_{1k}. Let's designate it as follows $m_1(\xi) = \sum_{k=-\infty}^{\infty} M_{1k} e^{i \frac{\pi}{L} k\xi}$;

$$\begin{aligned} m_1(\xi) = \frac{1}{2L} \times \\ \times \sum_{k=-\infty}^{\infty} \frac{\left(k_1 - V_1 \left(c\frac{\pi}{L}\right)^2 k^2\right) \left(c\frac{\pi}{L}\right)^2 k^2}{\left(\left(\frac{\pi}{L}\right)^2 k^2 - k_{1p}^2\right) \left(\left(\frac{\pi}{L}\right)^2 k^2 - k_{2p}^2\right)} \times \\ \times sinc^2 \left(\frac{\pi}{2L} k\right) e^{i \frac{\pi}{L} kx}. \end{aligned}$$

Details are presented in Appendix 1.

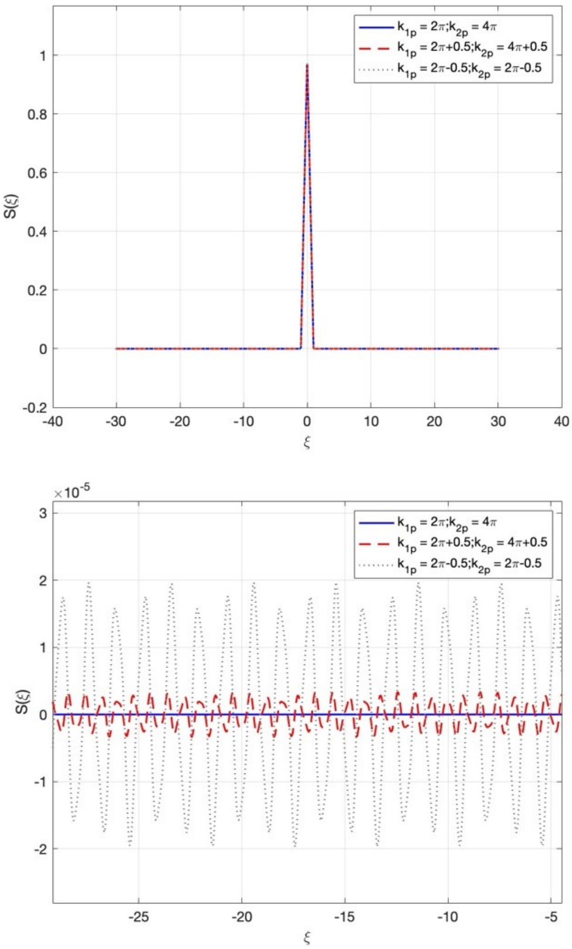

Figure 15. Spatial profiles for inner elements for the different parameters: the solid line corresponds to the anti-resonance condition, while the dotted and dashed lines show the modified parameters set

$$m_1(x) = \frac{1}{2L}\left(\frac{k_1 - c^2 V_1 {k_{2p}}^2}{{k_{2p}}^2 - {k_{1p}}^2}\right) * \\ *[-2|x|(sinc(k_{2p}x) - sinc(k_{1p}x)) + \\ + |x+1|(sinc(k_{2p}(x+1)) - sinc(k_{1p}(x+1))) + \\ + |1-x|(sinc(k_{2p}(1-x)) - sinc(k_{1p}(1-x)))].$$

Applying a complete Fourier transform of the equation $(10a)$, we obtain an integral equation of the convolution type

$$R(\xi) = \frac{1}{2L}\left(m_1 * R_+^p\right)(\xi). \qquad (11)$$

Considering the equation $(9b)$, we can express R_k and substitute it into the equation $(9a)$, then we get:

$$\left[k_1 + k_1 V_1 - c^2 V_1 \left(\frac{\pi}{L}\right)^2 k^2 - \frac{k_2 k_1}{c^2\left(\frac{\pi}{L}\right)^2 k^2} + k_2 V_1\right] S_k = \\ = \frac{k_1}{c^2} sinc^2\left(\frac{\pi}{2L}k\right)\left(R_+^p\right)_k.$$

Same as above, we will introduce the notation, then:

$$M_{2k} = \frac{k_1}{c^2}\frac{sinc^2\left(\frac{\pi}{2L}k\right)\left(R_+^p\right)_k}{\left(\left(k\frac{\pi}{L}\right)^2 - k_{1p}^2\right)\left(\left(k\frac{\pi}{L}\right)^2 - k_{2p}^2\right)} \\ S_k = M_{2k}\left(R_+^p\right).$$

$$S_k = M_{2k}\left(R_+^p\right). \qquad (12)$$

Let us proceed to the inverse transform for $M_{2k} m_2(\xi) = \sum_{k=-\infty}^{\infty} M_{2k} e^{i\frac{\pi}{L}k\xi}$

$$m_2(x) = \frac{1}{2L}\frac{k_1}{c^2}\times \\ \times \sum_{k=-\infty}^{\infty} \frac{\sin^2\left(\frac{\pi}{2L}k\right)e^{ikx}}{\left(\left(k\frac{\pi}{L}\right)^2 - k_{1p}^2\right)\left(\left(k\frac{\pi}{L}\right)^2 - k_{2p}^2\right)\left(k\frac{\pi}{L}\right)^2}.$$

Details are presented in Appendix 1.

$$m_2(x) = \frac{1}{2L}\frac{k_1}{c^2}[\frac{2}{k_{1p}^2 k_{2p}^2} max(1-|x|, 0) + \\ + \frac{1}{\left(k_{1p}^2 k\_2p^2\right)^2} * [-2|x|(sinc(k_{1p}x) - sinc(k_{2p}x)) + \\ + |x+1|(sinc(k_{1p}(x+1)) - sinc(k_{2p}(x+1))) + \\ + |1-x|(sinc(k_{1p}(1-x)) - sinc(k_{2p}(1-x)))]].$$

By applying a complete Fourier transform of the equation (12), we obtain an integral equation of the convolution type:

$$S(\xi) = \frac{1}{2L}\left(m_2 * R_+^p\right)(\xi). \qquad (13)$$

Figures 17(a) and 18(a) show the spatial profiles of the outer and inner elements, respectively. Figures 17(b) and 17(b) show graphs of the corresponding oscillating tails in magnification. As expected from theoretical considerations, there are no oscillating tails when the anti-resonance conditions are met: $k_1 = 2\pi n; k_2 = 2\pi m$ but with a slight detuning, they reappear.

6 Discussion and Conclusions

In our work we considered the model of the 1D locally resonant granular lattice on the elastic substrate. With the use of the numerical simulations, we observed two types of breathers, with in-phase and out-of-phase evolution of the inner and outer elements. The same way as in the case of mass-in-mass chains without substrate, the breathers can irradiate energy into the accompanying oscillatory tail. We use the approach of the inverse

Fourier transformation from the work by Xu et al.[Xu et al., 2015] to obtain the anti-resonance condition for the oscillatory tail to vanish. We consider the travelling waves in real space and demonstrate that the use of finite domains under non-resonance conditions may enable the convergence of the solution scheme. This approach gives us a complicated but valuable condition on the parameters of the system. This work could have some impact on the wave manipulation and control for the wider range of materials which represented by the discrete oscillatory models. The nonlinearity together with the local resonance phenomena can serve as a useful tool for the energy transport control and signal processing in many applications with different scales of realization, starting from micro- and up to macro-objects.

Acknowledgements

This work was supported by the Russian Science Foundation (project No. 24-23-00435).

References

Vakakis A.F., Gendelman O.V., Bergman L.A.et al.(2002). Nonlinear targeted energy transfer: state of the art and new perspectives. *Nonlinear Dyn.* , **108** pp. 711—741.

Vorotnikov K. ,Kovaleva M. and Starosvetsky Y.(2018). mergence of non-stationary regimes in one- and two-dimensional models with internal rotators. *Phil. Trans. R. Soc. A* , **376** p 20170134.

Manevitch L., Kovaleva A., Smirnov V.,Starosvetsky Yu. (2018). *Nonstationary Resonant Dynamics of Oscillatory Chains and Nanostructures*. Springer, Singapore.

Yacobi G.,Kislovsky V. , Kovaleva M., Starosvetsky Y.(2019). Unidirectional energy transport in the symmetric system of non-linearly coupled oscillators and oscillatory chains. *Nonlinear Dyn.* , **98** pp. 2687—2709.

ManevitchcL., Smirnov V., Romeo F.(2016). Unidirectional energy transport in the symmetric system of non-linearly coupled oscillators and oscillatory chains. *Cybernetics and Physics.* , **98** pp. 2687—2709.

Root / CYBERNETICS AND PHYSICS / Volume 5, 2016, Number 4 / Stationary and Non-stationary Resonance Dynamics of the Finite Chain of Weakly Coupled Pendula

Stationary and Non-stationary Resonance Dynamics of the Finite Chain of Weakly Coupled Pendula

Kapitula T., Promislow K. (2013). Spectral and Dynamical Stability of Nonlinear Waves. *Nonlinear Dyn.* , **98** Springer, New York.

Ma G. and Sheng P. (2016). Acoustic metamaterials: From local resonances to broad horizons. *Science Advances*, **2** p.1501595.

Haberman M.R., Guild M.D.. (2016). Acoustic metamaterials: By incorporating novel subwavelength structures into macroscopic materials, acousticians can create devices with exotic sound-altering properties. *Physics Today*, **69** pp.42–48.

Deng B., Raney J. R., Bertoldi K. , Tournat V. (2021). Nonlinear waves in flexible mechanical metamaterials. *J. Appl. Phys.*, **130** p.040901.

Roca D., Pàmies T., Cante J., Lloberas-Valls O., Oliver J. (2020). Experimental and Numerical Assessment of Local Resonance Phenomena in 3D-Printed Acoustic Metamaterials. *J. Vib. Acoust.*, **142** p.021017.

Zhou, Z., McFarland, D.M., Cheng, X. et al. (2023). One-dimensional granular chains as transmitted force attenuators. *Nonlinear Dyn.*, **111** pp.14713–14730.

Zega V., Silva P.B., Geers M.G.D,. et al.(2020). Experimental proof of emergent subharmonic attenuation zones in a nonlinear locally resonant metamaterial. *Sci Rep*, **10** p.12041.

Bashar Esmail A. F.(2022). Overview of Metamaterials-Integrated Antennas for Beam Manipulation Applications: The Two Decades of Progress. *IEEE Acces*, **10** pp.,96-99.

Gantzounis G., Serra-Garcia M., Homma K., Mendoza J. M., Daraio C.(2013). Granular metamaterials for vibration mitigation. *J. Appl. Phys.*, **114** p. 093514.

Smith D.R., Pendry J.B., Wiltshire M.C.K.(2004). Metamaterials and Negative Refractive Index . *Science*, **305** pp. 788-792.

Fang X., Lacarbonara W., Cheng L.,(2025). Granular metamaterials for vibration. *Nonlinear Dyn.*, **113** pp. 23787–23814.

Espinosa M., Calius E.P., Hall A. et al.,(2024). Pulse mitigation in ordered granular structures: from granular chains to granular networks. *Nonlinear Dyn.*, **112** pp. 15671–15699.

Bonanomi L., Theocharis G., Daraio C.,(2015). Wave propagation in granular chains with local resonances. *Phys. Rev. E*, **91** p. 033208.

Kevrekidis P., Vainchtein A., Garcia M. , Daraio C.,(2013). Interaction of traveling waves with mass-with-mass defects within a Hertzian chain. *Phys. Rev. E*, **91** p. 033208.

Banerjee A., Das R., Calius E.P.,(2019). Waves in structured mediums or metamaterials: a review. *Archives of Computational Methods in Engineering*, **26** pp. 1029-1058.

Huang H. H., Sun C. T., Huang G.L. ,(2009). On the negative effective mass density in acoustic metamaterials. *International Journal of Engineering Science*, **47** pp. 610.

P. Rosenau, A. Pikovsky,(2014). Breathers in strongly anharmonic lattices. *Phys. Rev. E.*, **89** p.022924.

Kikot I.K., Rayzan N.B., Kovaleva M., Starosvetsky Y.,(2022). Discrete breathers and discrete oscillating kink solution in the mass-in-mass chain in the state of acoustic vacuum. *Comm. in Nonl. Sci.and Num. Simul.*, **107** p. 106020.

Porubov A.V. (2023). Continuum Description of Extended Mass-in-Mass Metamaterial Models. In *Proc. Int. Symp. Electromagn. Compat.*, Altenbach, H., Berezovski, A., dell'Isola, F., Porubov, A. (eds) Sixty Shades of Generalized Continua. *Advanced Structured Materials,* , **170** Springer, Cham.

Jayaprakash K.R., Vakakis A.F., Starosvetsky Y.,(2013). Strongly nonlinear traveling waves in granular dimer chains. *Mechanical Systems and Signal Processing*, **39** pp. 91-107.

Starosvetsky Y., Jayaprakash K.R., Vakakis A.F., ,(2017). Traveling and solitary waves in monodisperse and dimer granular chains. *Journal of Modern Physics B*, **31** pp. 1742001.

G. James ,(2012). Periodic travelling waves and compactons in granular chains. *J. Nonlinear Sci.*, **22** pp. 813-848.

James G., Kevrekidis P.G. and Cuevas J. ,(2013). Breathers in oscillator chains with Hertzian interactions. *Physica D*, **251** pp. 39-59.

Kevrekidis P. G.,Stefanov A. G. , and Xu H.,(2016). Traveling waves for the mass-in-mass model of granular chains. *Lett. Math. Phys.*, **106** p.1067.

Xu H., Kevrekidis P. G.,Stefanov A. G. ,(2015). Traveling Waves and Their Tails in Locally Resonant Granular Systems. *Phys. Rev. E.*, **92** p.042902.

Liu L., James G., Kevrekidis P. G., and Vainchtein A. ,(2016). Strongly nonlinear waves in locally resonant granular chains. *Nonlinearity*, **29** p.3496.

Wallen S. P., Lee J. , Mei D., Chong C., Kevrekidis P. G., and Boechler N.,(2017). Discrete breathers in a mass-in-mass chain with Hertzian local resonators. *Phys. Rev. E*, **95** p.022904.

Liu L., James G., Kevrekidis P. G., and Vainchtein A. ,(2016). Breathers in a locally resonant granular chain with precompression. *Physica D, **331** p.27.*

Bonanomi L., Theocharis G., and Daraio C.,(2015). Wave propagation in granular chains with local resonances. Phys. Rev. E, **91** p.033208.

Vorotnikov K., Starosvetsky Y., Theocharis G., Kevrekidis P.G.,(2018). Wave propagation in granular chains with local resonances. *Physica D, **365** pp.27-41.*

James G.,(2012). Nonlinear waves in Newton's cradle and the discrete p-schoedinger equation. Models and Methods in Applied Sciences, **21** pp. 2335–2377.

Starosvetsky Y., Hasan M.A., Vakakis A.F., Manevitch L.I.,(2012). Strongly nonlinear beat phenomena and energy exchanges in weakly coupled granular chains on elastic foundations. *SIAM Journal on Applied Mathematics, **72** pp. 337-361.*

Hasan M.A., Starosvetsky Y., Vakakis A.F., Manevitch L.I.,(2013). Nonlinear targeted energy transfer and macroscopic analog of the quantum Landau–Zener effect in coupled granular chains. Physica D, **252** pp. 337-361.

Bukhari M.A., Barry O.R., Vakakis A.F.,(2023). Breather Propagation and Arrest in a Strongly Nonlinear Locally Resonant Lattice . *Mechanical Systems and Signal Processing, **252** pp. 337-361.*

Wattis A. D. J.,(2022). Breather modes of fully nonlinear mass-in-mass chains. Phys. Rev. E, **105** p.054212.

Hasan M.A., Cho S., Remick K. et al.,(2015). Experimental study of nonlinear acoustic bands and propagating breathers in ordered granular media embedded in matrix. *Granular Matter, **17** pp. 49–72.*

English J. M. , Pego R. L.,(2005). On the solitary pulse in a chain of beads. Proceedings of the American Mathematical Society, **133** pp. 1763–1768

Al. Mojahed, Al. F. Vakakis,(2020). Certain Aspects of the Acoustics of a Strongly Nonlinear Discrete Lattice. *Nonlinear Dyn., **133** pp. 643-659.*

Liu L., Hussein M.I.,(2012). Wave Motion in Periodic Flexural Beams and Characterization of the Transition Between Bragg Scattering and Local Resonance. J. Appl. Mech., **79** p. 01100.

Stefanov A. and Kevrekidis P.G.,(2012). On the existence of solitary traveling waves for generalized Hertzian chains. *J. Nonlin. Sci, **22** 327–349.*

Kim E., and Chaunsali R., and Xu H., and Jaworski J., and Yang J. , and Kevrekidis P. G., and Vakakis A. F.,(2015). Nonlinear low-to-high-frequency energy cascades in diatomic granular crystals. Phys. Rev. E, **92** 062201

Appendix A Head of an Appendix

$$m_1(\xi) = \frac{1}{2L}\times$$
$$\times\sum_{k=-\infty}^{\infty}\frac{\left(k_1 - V_1\left(c\frac{\pi}{L}\right)^2 k^2\right)\left(c\frac{\pi}{L}\right)^2 k^2}{\left(\left(\frac{\pi}{L}\right)^2 k^2 - k_{1p}^2\right)\left(\left(\frac{\pi}{L}\right)^2 k^2 - k_{2p}^2\right)}\times$$
$$\times sinc^2\left(\frac{\pi}{2L}k\right)e^{i\frac{\pi}{L}kx}.$$

Let's divide it into two terms and introduce the notation: $\frac{\pi}{L}k = \widetilde{k}$, we will omit the tilde below.

$$m_1(\xi) =$$
$$= \frac{2k_1}{L}\sum_{k=-\infty}^{\infty}\frac{\sin^2\left(\frac{k}{2}\right)e^{ikx}}{\left(k^2 - k_{1p}^2\right)\left(k^2 - k_{2p}^2\right)} -$$
$$-\frac{2c^2V_1}{L}\sum_{k=-\infty}^{\infty}\frac{\sin^2\left(\frac{k}{2}\right)e^{ikx}}{\left(k^2 - k_{1p}^2\right)\left(k^2 - k_{2p}^2\right)}.$$

Next, let's break it down into elementary fractions:

$$m_1(\xi) = \frac{2k_1}{L}\sum_{k=-\infty}^{\infty}\frac{1}{\left(k_{2p}^2-k_{1p}^2\right)}\times$$
$$\times\left(\frac{\sin^2\left(\frac{k}{2}\right)e^{ikx}}{(k-k_{2p})(k+k_{2p})}-\frac{\sin^2\left(\frac{k}{2}\right)e^{ikx}}{(k-k_{1p})(k+k_{1p})}\right)-$$
$$-\frac{2c^2V_1}{L}\frac{k_{2p}^2}{\left(k_{2p}^2-k_{1p}^2\right)}\times$$
$$\times\left(\frac{\sin^2\left(\frac{k}{2}\right)e^{ikx}}{(k-k_{2p})(k+k_{2p})}-\frac{\sin^2\left(\frac{k}{2}\right)e^{ikx}}{(k-k_{1p})(k+k_{1p})}\right)$$

Let's rewrite separately

$$m_1(\xi) = m_a(\xi) + m_b(\xi).$$

Knowing [4] that

$$F^{-1}\left[\frac{\sin\left(\frac{k-k_0}{2}\right)}{\left(\frac{k-k_0}{2}\right)}\frac{\sin\left(\frac{k+k_0}{2}\right)}{\left(\frac{k+k_0}{2}\right)}\right]=$$
$$=2|x|\,sinc(k_0x)+$$
$$+|x+1|\,sinck_0(x+1)+$$
$$+|1-x|\,sinck_0(1-x).$$

Let us consider the first component:

$$m_a(\xi) = \frac{2k_1}{4L}\sum_{k=-\infty}^{\infty}\frac{1}{\left(k_{2p}^2-k_{1p}^2\right)}\times$$
$$\left[\frac{\sin\left(\frac{k-k_{2p}}{2}\right)\sin\left(\frac{k+k_{2p}}{2}\right)e^{ikx}}{\left(\frac{k-k_{2p}}{2}\right)\left(\frac{k-k_{2p}}{2}\right)}-\right.$$
$$\left.-\frac{\sin\left(\frac{k-k_{1p}}{2}\right)\sin\left(\frac{k+k_{1p}}{2}\right)e^{ikx}}{\left(\frac{k-k_{1p}}{2}\right)\left(\frac{k-k_{1p}}{2}\right)}.\right.$$

Let us consider the first component:

$$m_a(\xi) = \frac{k_1}{2L}\frac{1}{{k_{2p}}^2-{k_{1p}}^2}[2|x|\,(sinc(k_{2p}x)-sinc(k_{1p}x))+$$
$$+|x+1|\,(sinc(k_{2p}(x+1))-sinc(k_{1p}(x+1)))+$$
$$++|1-x|\,(sinc(k_{2p}(1-x))-sinc(k_{1p}(1-x)))].$$